

Design, construction and experimental observation of a thermoacoustic prime mover

By

J.G.B. Jacobs

in partial fulfilment of the requirements for the degree of

Master of Science

Sustainable Process and Energy Technologies

at the Delft University of Technology,
to be defended on Friday December 12, 2014

Supervisor:

prof. dr. ir. B.J. Boersma

Abstract

In this study a thermoacoustic single stage engine configuration is compared to a double stage engine configuration with regard to onset temperature, power density and efficiency. A thermoacoustic prime mover was designed and build using air at 1 atmosphere as a working fluid. The ceramic regenerators were heated using electricity and cooled using cooling water. Pressure and temperature measurements are done at several locations in the engine. It has been shown that acoustic energy can be converted into electric power with the use of a linear alternator. It has also been shown that the double stage engine operates at a lower working temperature. It produces more electric power and thus obtains a higher power density than the single stage thermoacoustic engine. Measurements show the onset temperature of the single and double stage engine are respectively 303 °C and 267 °C. However, 2nd law efficiencies for single stage configuration are at least 34% higher than efficiencies for double stage configuration. An electric output power of 0.79 W is realized at an overall efficiency of 0.28%.

Contents

Nomenclature.....	6
List of Figures.....	7
1. Introduction.....	8
1.2 Brief history.....	10
2.1 Stirling cycle.....	12
2.1.1 Prime mover.....	12
2.1.2 Heat pump.....	14
2.3 Standing wave systems.....	16
2.3.1 Prime mover.....	16
2.3.2 Temperature gradient.....	17
2.3.3 Heat pump or prime mover.....	18
2.3.4 Stack.....	19
2.4 Travelling wave systems.....	19
2.5 Standing versus travelling wave systems.....	20
2.5.1 Sound pressure.....	22
2.5.2 Pressure ratio.....	23
2.5.3 Linearity.....	23
3. Design.....	24
3.1 Requirements.....	24
3.2 Parts.....	25
3.2.1 Tube specifications.....	25
3.2.2 Regenerator.....	25
3.2.3 Hot heat exchanger.....	26

3.2.4 Cold heat exchanger.....	26
3.2.5 Regenerator tube.....	27
3.2.6 Stub.....	27
3.2.7 Alternator	28
3.3 Construction	29
3.3.2 Regenerator tube.....	29
3.3.1 Regenerator	30
3.3.3 Hot heat exchanger.....	30
3.3.4 Cold heat exchanger.....	31
3.3.5 Assembly	31
4. Experimental results	33
4.1 Experimental setup.....	33
4.2 Data acquisition.....	33
4.2.1 Temperature measurements	33
4.2.2 Acoustic pressure measurements.....	33
4.2.3 Electric power output and efficiency.....	34
4.3 Results.....	35
4.3.1 Single stage prime mover	35
4.3.1.1 Temperature	35
4.3.1.2 Pressure.....	37
4.3.2 Single stage versus double stage prime mover.....	39
5. Conclusions and recommendations.....	42
Bibliography.....	43

Nomenclature

Roman

A	Area
c	Specific heat
COP	Coefficient of performance
$COPC$	Carnot COP
$COPR$	COP relative to the Carnot COP
E	Energy
k	Thermal conductivity
P	Pressure
p	Acoustic pressure
Pr	Prandtl number
pr	Pressure ratio
Q	Heat
R	Resistance
r_h	Hydraulic radius
S_{iso}	Entropy of an isolated system
SPL	Sound pressure level
T	Temperature
U	Voltage
V	Volume
v	Velocity
W	Work
w	Velocity amplitude

Greek

α	Thermal diffusivity
δ	Penetration depth
η	Efficiency
μ	Dynamic viscosity
Π	Wetted perimeter
ρ	Density
ω	Radial frequency

Subscripts

$2nd$	Second
c	Cold
$carnot$	Carnot
ch	Channel
$crit$	Critical
el	Electric
hp	Heat pump
iso	Isolated system
m	Mean
p	Constant pressure
$pore$	Pore
κ	Thermal
ref	Refrigerator
$refer$	Reference
rms	Root mean square
t	Tube
w	Water

List of Figures

Figure 1.1	<i>World total energy consumption, 1820-2010 and 1990-2040</i>	8
Figure 1.2	<i>Travelling wave engine with using solar heat to produce electrical power</i>	9
Figure 1.3	<i>Schematic representation of the Rijke tube, Leiden, 1859</i>	10
Figure 1.4	<i>Hoflors standing wave refrigerator</i>	11
Figure 1.5	<i>Schematic representation of the travelling wave engine by Backhaus and Swift</i>	11
Figure 2.1	<i>Stirling cycle with four steps</i>	12
Figure 2.2	<i>Schematic pV diagram and TS-diagram of a Stirling cycle</i>	13
Figure 2.3	<i>Illustration of a prime mover converting heat from the hot reservoir into work</i>	15
Figure 2.4	<i>Schematic representation of the Sondhauss tube, 1850</i>	16
Figure 2.5	<i>Schematic pV diagram and TS-diagram of a Brayton cycle</i>	16
Figure 2.6	<i>Standing wave in a one sided closed tube</i>	17
Figure 2.7	<i>The first thermoacoustic travelling wave engine made by Ceperley, 1979</i>	19
Figure 2.8	<i>Four stages of a travelling thermoacoustic engine</i>	20
Figure 2.9	<i>Plot of pressure and velocity for a travelling acoustic wave as a function of time</i>	22
Figure 2.10	<i>Plot of pressure and velocity for a standing acoustic wave as a function of time</i>	22
Figure 3.1	<i>Ceramic catalyst used as regenerator material</i>	26
Figure 3.2	<i>Illustration of a thermoacoustic system with the implementation of a stub</i>	28
Figure 3.3	<i>Drawings of the regenerator tube</i>	29
Figure 3.4	<i>Assembly of the second regenerator tube</i>	30
Figure 3.5	<i>Construction of the hot heat exchanger</i>	30
Figure 3.6	<i>Construction of the cold heat exchanger</i>	31
Figure 3.7	<i>Dimensions and way of assembly of the thermoacoustic prime mover</i>	32
Figure 4.1	<i>Experimental setup in single stage configuration and double stage configuration</i>	33
Figure 4.2	<i>Schematic illustration of the experimental setup</i>	34
Figure 4.3	<i>Temperature at both sides of the regenerator as a function of time at 44 Watts heat</i>	36
Figure 4.4	<i>Onset pressure deviation from the ambient atmospheric pressure</i>	37
Figure 4.5	<i>Pressure waves at different points in the engine at an input of 80 Watts</i>	38
Figure 4.6	<i>Power spectrum at an input of 80 Watts with a partially closed resonator</i>	38
Figure 4.7	<i>Temperature onset behaviour of the double stage prime mover</i>	39
Figure 4.8	<i>Electric power output as a function of total heat input</i>	40
Figure 4.9	<i>Overall efficiency as a function of total heat input</i>	40

1. Introduction

Population growth and the world's increased living standard have led to an increase of the world energy consumption. The total energy use in 2013 has been nine times the energy use of 1914 [18]. The trend continues, the American Energy Information Administration (EIA) projects that world energy consumption will grow by 56% between 2010 and 2040 as shown in figure 1.1. This growth mostly occurs in countries outside the Organization for Economic Cooperation and Development (OECD). Energy use in non-OECD countries will increase by 90 percent and in OECD countries by 17 percent [16]. Currently the industry accounts for the largest share of the world's energy consumption. By further increase of the living standard the energy use in this sector will increase tremendously due to increasing customer needs. As the EIA projects the industrial sector continues to account for the largest share of delivered energy consumption in 2040. This corresponds to a CO₂ emission rise from about 31 billion metric tons in 2010 to 45 billion in 2040, a 46-percent increase.

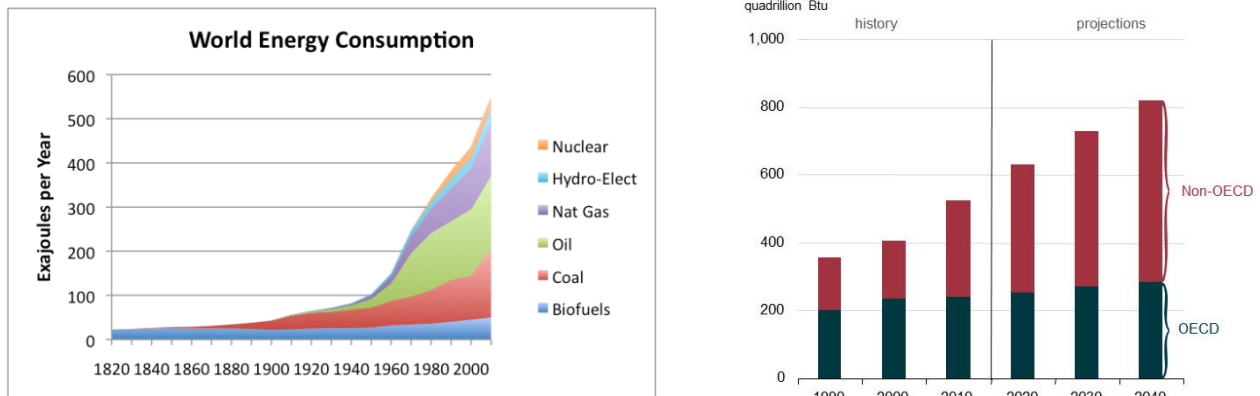


Figure 1.1: World total energy consumption, 1820-2010 [18] and 1990-2040 [16].

To provide the future world with this amount of energy more power plants are needed. But since greenhouse gases like CO₂ may contribute to global warming and the availability of fossil fuels is limited, alternative energy sources have to be explored and developed. Sustainable energy sources can be found in the form of wind power, water power, geothermal power and solar power. Solar energy is one of the most investigated

forms of sustainable energy. One technology is concentrated solar power (CSP), a system that uses mirrors to concentrate a large area of sunlight onto a small area and convert the heat into electricity. For this step often a Stirling engine is used. Stirling engines are most of the time piston engines which are highly efficient but have several disadvantages like production costs and maintenance. Instead of a Stirling engine a thermoacoustic engine can be used.

In figure 1.2 a 2014 thermoacoustic CSP system is shown. A large dish aimed at the sun reflects the light rays into the focus point, where the hot source of the thermoacoustic engine is located. The heat is converted into acoustic energy which is converted into electricity with the use of linear alternators. Up to 1 kW of electrical power can be generated with the use of this system [19].



Figure 1.2: *Travelling wave thermoacoustic engine with using solar heat to produce electrical power made by Qnergy, Utah.*

Thermoacoustic is a field that still requires a lot of research. It describes the relation between thermodynamics and acoustics. Very brief explained, a temperature gradient in an enclosed space can be used to generate acoustic waves which can be used to generate electricity. Several benefits of thermoacoustic engines are they contain no moving parts, have an environmentally friendly working medium and are reliable and relatively cheap [17]. Other can be found in spacecraft, electronics and energy sectors in the form of cooling and in the industry in the form of waste heat recovery.

1.2 Brief history

The thermoacoustic effect was discovered centuries ago by glass blowers [1]. Glass blowers used a long cold tube containing a hot glass bulb on the far end which spontaneously produced a monotone sound. The first scientific work was done in the eighteenth century by Higgins [2], creating the singing flame by burning hydrogen in an open vertical tube. These experiments were followed up by Rijke [3], replacing the flame by a hot wire mesh creating the Rijke tube, presented in figure 1.3. When the wire mesh was placed at $\frac{1}{4}$ of the pipe length, the sound production was found to be optimal.

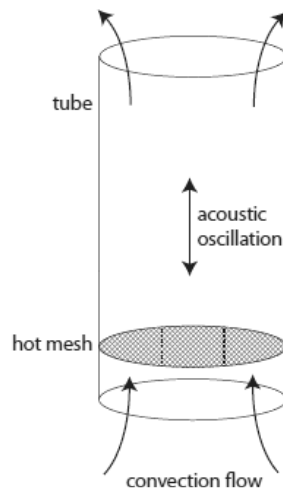


Figure 1.3: Schematic representation of the Rijke tube, Leiden, 1859. A convective air flow through the tube is necessary to keep the oscillation running.

In 1850 Sondhauss used a long, small diameter tube with a bulb on the far end similar as the glass blowers tube. When enough heat was supplied to the bulb a monotone sound was generated. Sondhauss experiments showed this tones frequency was dependent of the length of the tube and the volume enclosed by the bulb.

The theoretic explanations of these results came over a century later from Lord Rayleigh [4], as he stated:

“If heat be given to the air at the moment of greatest condensation or taken from it at the moment of greatest rarefaction, the vibration is encouraged.”

This qualitative understanding shows Rayleigh related thermoacoustics to the interplay of density variations and heat injection.

The breakthrough came when Rott in 1969 presented a linear theory in the study thermoacoustics. He developed the mathematics describing the acoustic oscillations of a tube with its diameter much smaller than its wavelength [7]. This mathematical understanding is still the base for thermoacoustic modeling today.

Rott's work led to the production of numerous thermoacoustic test devices. Later on Hofler created with success a standing wave refrigerator (shown in figure 1.4), using a sound wave produced by a speaker to create a temperature gradient over a stack so that heat was pumped from the low temperature side to the hot temperature side [8]. Hofler's refrigerator proved that Rott's mathematical description was correct.

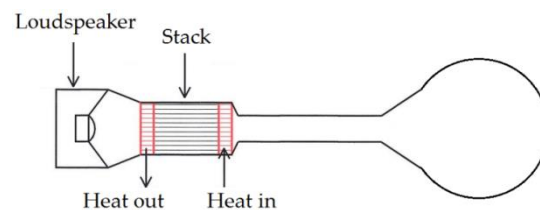


Figure 1.4: Hoflers standing wave refrigerator. A loudspeaker is used to create a temperature gradient over a stack, pumping heat against the temperature gradient.

Thermoacoustics became a widely researched topic at many universities and research centers. An important discovery was done by Ceperley in 1979. He found out that looped thermoacoustic devices could be related to the Stirling cycle, a thermodynamic cycle achieving higher efficiencies than thermoacoustic systems so far. Later on Backhaus and Swift at the Los Alamos National Laboratory successfully build a high efficient thermoacoustic travelling wave prime mover using a looped tube with a long resonator tube, reducing velocity and therefore friction losses in the loop (shown in figure 1.5). Swift summarized his findings together with Rott's work and a detailed thermodynamic explanation [9].

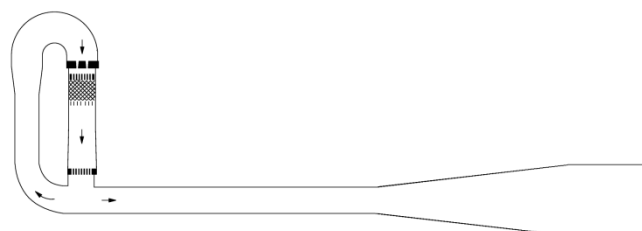


Figure 1.5: Schematic representation of the highly efficient travelling wave thermoacoustic engine by Backhaus and Swift, 2000.

2. Theory

In this chapter the thermoacoustic theory is explained along with its thermodynamic background. First a thermodynamic cycle is discussed, the Stirling cycle. This cycle forms the base of the most efficient thermoacoustic systems: travelling wave systems. Here thermodynamic quantities as second law efficiency and COP are introduced. In the next part standing wave systems are introduced. Here the thermoacoustic effect is described along with the introduction of the stack. Afterwards traveling wave systems are described relating the Stirling cycle to thermoacoustics. Finally the distinction between traveling and standing wave systems are discussed.

2.1 Stirling cycle

2.1.1 Prime mover

In the figure below a Stirling engine is presented at four stages of the cycle. A Stirling engine is a closed energy conversion system, converting heat into mechanical work. Its starting position is shown in figure 2.1a. Cold air is compressed, transferring heat to the walls of the cylinder. The compressed gas flows into the hot cylinder at 2.1b where the gas is heated. The hot gas is expanding, moving the upper piston downwards (2.1c), where work is delivered to the crankshaft. Heat is removed from the gas at the upper cylinder (2.1d) as the cycle starts again by compressing the cold gas.

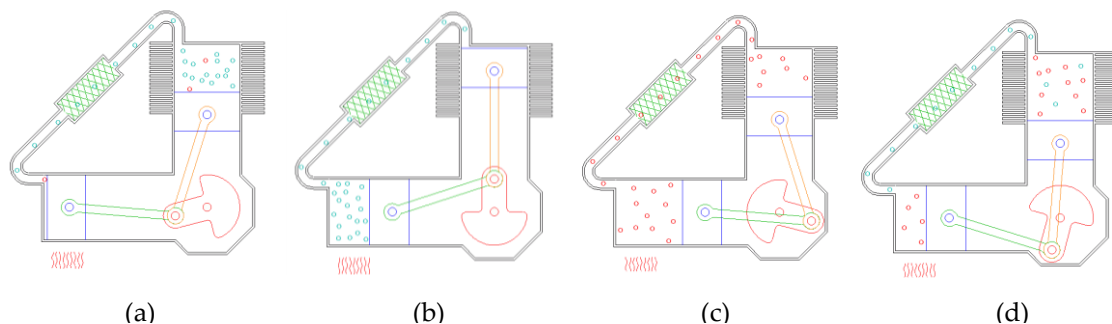


Figure 2.1: Stirling cycle with four steps, isothermal compression (a) isochoric heat addition (b) isothermal expansion (c) isochoric heat removal (d).

To increase the efficiency a regenerator is installed coloured green in figure 2.1. This is a regenerative heat exchanger often made of a metal foam which functions as a heat sponge. When the hot gas flows to the cold cylinder it passes the regenerator which stores the heat from the fluid intermittently. The cold fluid absorbs the heat when it is returning to the hot cylinder. Without a regenerator this amount of heat would flow directly from hot to cold heat exchanger, decreasing the systems efficiency dramatically.

In figure 2.2 the ideal thermodynamic cycle of the Stirling engine is shown. Heat is added when the gas flows through the regenerator and when it is expanding into the hot cylinder. Heat is removed when the gas is flowed back through the regenerator and compressed in the hot cylinder. The difference between the amount of heat in and out of the system is the amount of work produced in the cycle, equal to the area enclosed in the pV-diagram:

$$W = Q_{in} - Q_{out} = \int_{V_i}^{V_f} PdV . \quad (1.1)$$

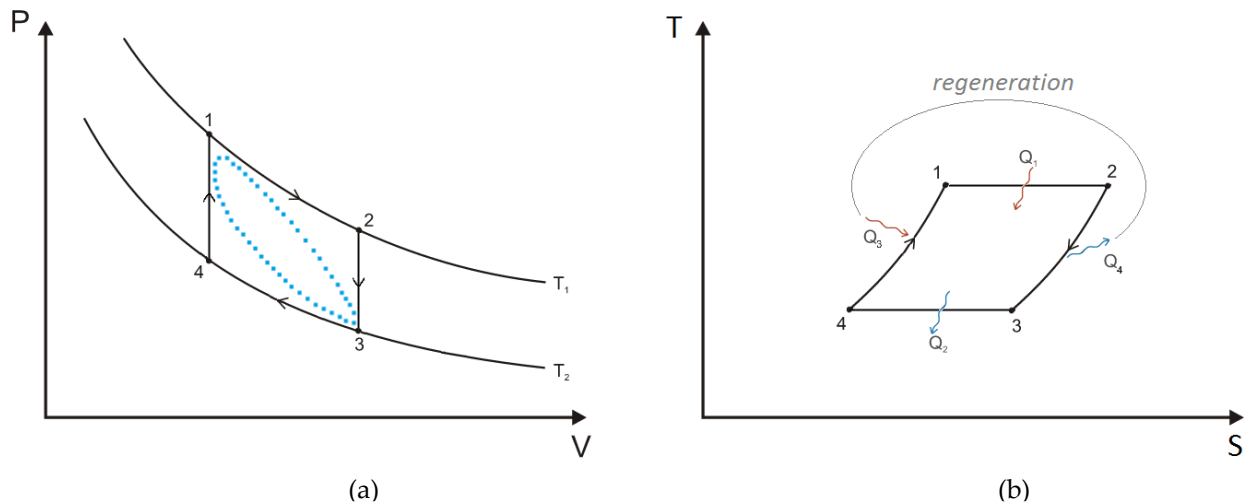


Figure 2.2: Schematic pV diagram (a) and TS-diagram (b) of a Stirling cycle. 1-2: isothermal expansion, 2-3: isochoric heat removal, 3-4: isothermal compression, 4-1: isochoric heat addition.

The blue dots in figure 2.2 indicate a cycle that is a more realistic representation of a real Stirling engine. The enclosed area of the blue dots is much smaller than in the ideal cycle due to losses which result in an efficiency smaller than 100%.

The second law of thermodynamics states that the entropy of an isolated system never decreases, because an isolated systems always evolves toward a state with maximum entropy:

$$\dot{S}_{iso} \geq 0. \quad (1.2)$$

With entropy mathematically defined as:

$$dS = \frac{\delta Q}{T}. \quad (1.3)$$

The efficiency of the cycle relates the amount of work produced for a given amount of heat energy input:

$$\eta = \frac{\dot{W}}{\dot{Q}}. \quad (1.4)$$

The efficiency is bounded by the Carnot limit. Using the second law of thermodynamics:

$$\eta_{carnot} = 1 - \frac{T_c}{T_H}. \quad (1.5)$$

To compare efficiencies of engines working at different temperature differences, the second law efficiency is introduced. Since the thermoacoustic engine is theoretically a reversible heat engine, the maximum useful work possible during a cycle equals the exergy. The exergy of a system is the maximum useful work during a process that brings the system into equilibrium with its surroundings [21]. The second law efficiency equals the engines efficiency divided by its theoretical maximum. It is illustrated in figure 2.2 as the enclosed blue cycle divided by the ideal cycle:

$$\eta_{2nd} = \frac{\eta}{\eta_{carnot}} \quad (1.6)$$

2.1.2 Heat pump

In 2.1.1 the thermoacoustic effect in terms of converted heat into work is discussed. However, the cycle can also be used the other way around. Acoustic energy can be used to pump heat against a temperature gradient as illustrated in figure 2.3b. If the goal is to cool an environment, the system is named a refrigerator. If the goal is to

heat an environment, the system is named a heat pump. The performance of the refrigerator or heat pump is described using the coefficient of performance (COP) which is defined as follows:

$$COP_{ref} = \frac{\dot{Q}_c}{\dot{W}}, \quad (1.7)$$

$$COP_{hp} = \frac{\dot{Q}_c + \dot{W}}{\dot{W}}. \quad (1.8)$$

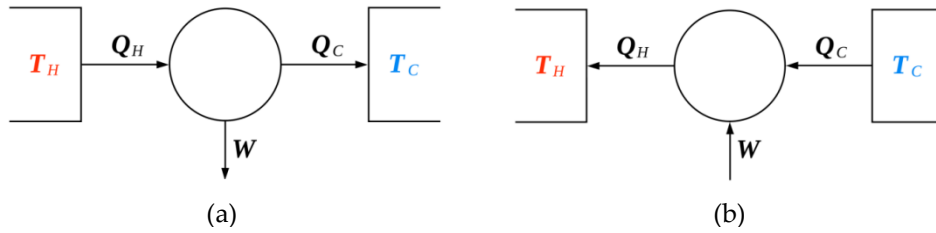


Figure 2.3: Illustration of a prime mover converting heat from the hot reservoir into work rejecting waste heat to the cold reservoir (a), and a heat pump using work to pump heat from the cold to the hot reservoir (b).

The COP is bounded by the second law of thermodynamics. The maximum COP is temperature dependent and defined as:

$$COPC_{ref} = \frac{T_c}{T_H - T_c}, \quad (1.9)$$

$$COPC_{hp} = \frac{T_H}{T_H - T_c}. \quad (1.10)$$

The COP relative to the Carnot COP is defined as:

$$COPR = \frac{COP}{COPC}. \quad (1.11)$$

2.3 Standing wave systems

2.3.1 Prime mover

In this section the first of the two wave systems is discussed: standing wave systems. One of the first thermoacoustic test setups came from Sondhauss. The air filled Sondhauss tube is shown in figure 2.4, a tube with a hot bulb on the end.

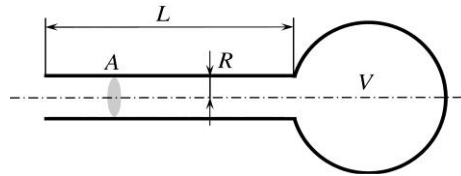


Figure 2.4: Schematic representation of the Sondhauss tube, 1850

When heat is added to the bulb the increase in gas pressure inside the bulb causes the gas to flow towards the opening of the cold tube. The gas exiting the tube forces the outside air aside, creating a sound wave in the outside air. Since the gas in the cold tube has dropped in temperature, its pressure is lowered and the atmosphere presses the gas back into the tube. The gas flows towards the hot bulb heating up increasing in pressure and the cycle starts again. The cycle of this standing wave system is related to the Brayton cycle, presented in figure 2.5. The working gas in the engine is compressed adiabatically, then heat is transferred at constant pressure, then the working gas expands adiabatically and heat is rejected at constant pressure returning to the first step.

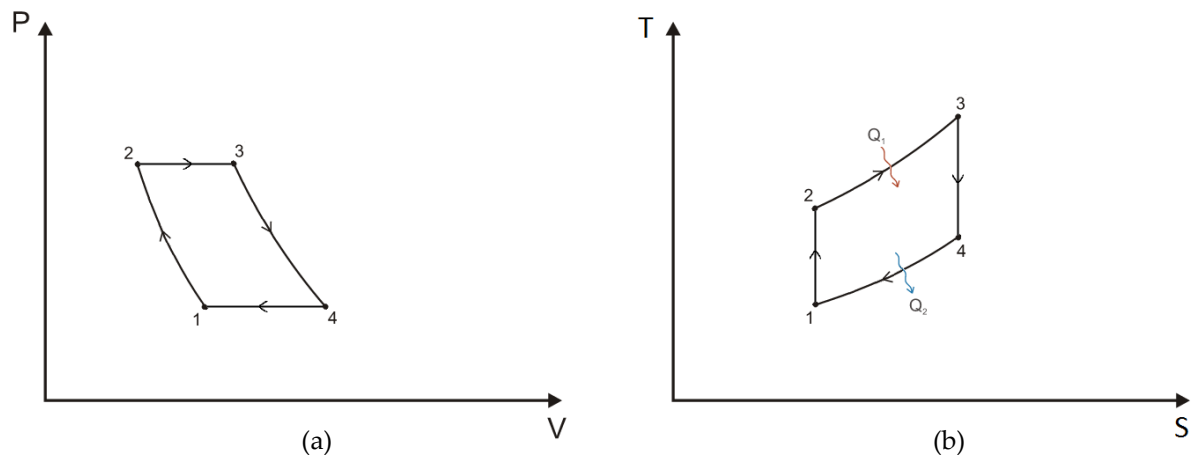


Figure 2.5: Schematic pV diagram (a) and TS -diagram (b) of a Brayton cycle. 1-2: adiabatic compression, 2-3: isobaric heat addition, 3-4: adiabatic expansion, 4-1: isobaric heat removal.

2.3.2 Temperature gradient

The Sondhauss tube is simplified to a long tube closed on one end as in figure 2.6a. In the tube a standing wave is generated with a velocity node at the closed end since no gas is oscillating at the wall, and a velocity antinode at open end since there are large gas displacements in the open air. In 2.6b these velocity oscillations of the tube are plotted as the red curve as a function of location at a specific time. The antinode at the open end and node at the closed end are clearly visible.

The pressure variations are also plotted in this graph as the blue curve. As an opposite of the red curve, the pressure graph contains a pressure node at the open end since the atmospheric pressure is constant and an antinode at the closed end since the particles are not moving and experiencing large pressure oscillations.

Under isentropic conditions these pressure oscillations are accompanied by large temperature oscillations. These temperature oscillations are dependent of the x - location and its slope is called the temperature gradient. The temperature gradient at four specific locations is presented at the bottom of 2.6b. At the opening of the tube the pressure is atmospheric, air will flow in and out freely resulting in a velocity antinode and a pressure node. Since there are no pressure changes temperature changes are absent and the temperature gradient is flat. At the closed end of the tube there is no flow, the molecules stay in place experiencing large pressure oscillations and therefore temperature oscillations. Here the temperature gradient is very steep.

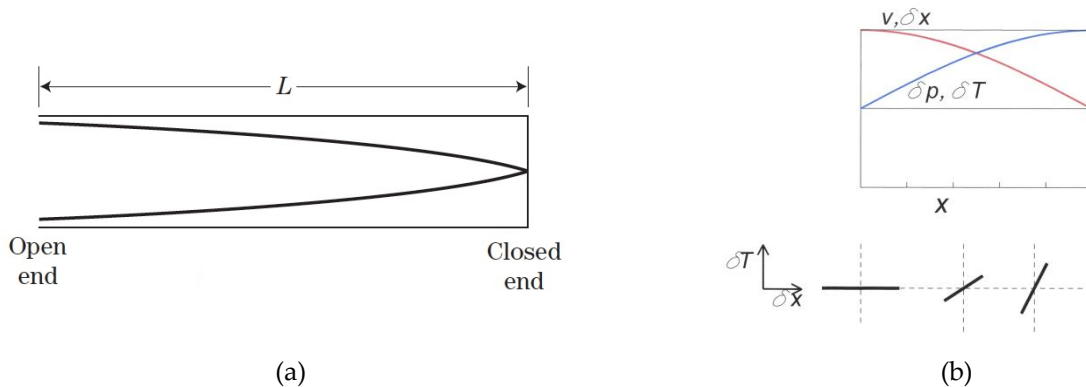


Figure 2.6: Standing wave in a one sided closed tube (a) and a plot of the pressure and temperature variations and the corresponding plots inside the tube (b).

For the thermoacoustic effect to occur both velocity oscillations and a large temperature gradient are needed, a specific situation which can be found at the location of one quarter of the length of the pipe. The gradient of the gas molecules at this location is defined as “the critical temperature gradient” and is dependent on certain characteristics of the pipe as frequency, cross sectional area and gas properties [9]:

$$\nabla T_{crit} = \frac{\omega A |p|}{\rho_m c_p |w|} \quad (1.12)$$

with ω the radial frequency, A the cross-sectional area, $|p|$ and $|w|$ the acoustic pressure and velocity amplitude and ρ_m and c_p the mean density and thermal heat capacity of the gas. When installed at the right location in a prime mover the temperature gradient is connected to efficiency and output power. The steeper the gradient, the higher the Carnot efficiency and thus the acoustic power. If the gradient is equal to the critical temperature gradient, no heat is converted into acoustic power. When the temperature gradient is smaller than the critical temperature gradient, acoustic energy is used to increase the temperature gradient as discussed in the section below.

2.3.3 Heat pump or prime mover

If the temperature gradient of the wall is smaller than the critical temperature gradient of the gas, acoustic power will be used to pump heat against the temperature gradient of the wall. The temperature gradient will get steeper. Heat can be extracted at the hot side of the regenerator, while a cold stream can be cooled at the cold side of the regenerator. This system functions as a heat pump or refrigerator.

If the wall temperature exceeds the critical temperature gradient, the gas molecules receive heat when they are compressed end and transfer heat when they are expanded. Heat is turned into acoustic power amplifying the wave. This system functions as a prime mover.

2.3.4 Stack

To increase the power density of the system more wall area has to be provided. A porous medium like a parallel placed plate geometry can be used to increase the amount of contact between the wall and the working gas. This porous medium is called a stack for standing wave systems and a regenerator for travelling wave systems further explained in section 2.4. Stacks and regenerators are enclosed by a hot and a cold heat exchanger to maintain the temperature gradient over the porous medium, or to pump heat from the cold to the hot heat exchanger.

2.4 Travelling wave systems

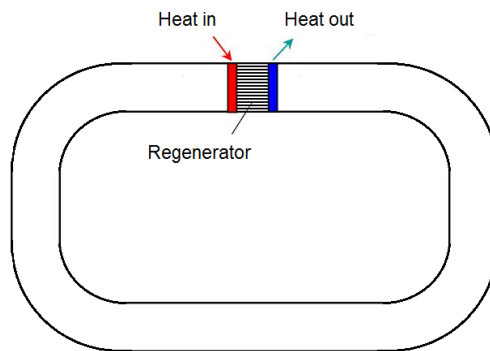


Figure 2.7: *The first thermoacoustic travelling wave engine made by Ceperley, 1979*

The second wave system are traveling wave systems. A simple system is shown in figure 2.7. It presents a looped tube containing a hot heat exchanger, a regenerator and a cold heat exchanger. The regenerator is sandwiched between both heat exchangers so a temperature gradient across the regenerator arises. Both heat exchangers and the regenerator contain pores so gas can vibrate in longitudinal direction. There is basically no net flow inside the looped tube, there are only oscillations, molecules being pushed forwards and backwards transporting a wave counter clockwise through the tube.

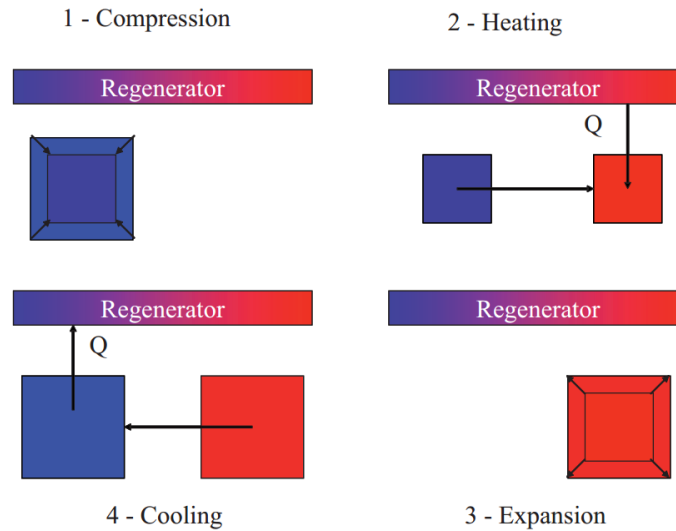


Figure 2.8: Four stages of a travelling wave thermoacoustic engine.

Travelling wave systems are related to the Stirling cycle with its compression and expansion caused by an acoustic wave. As in figure 2.8, the wave arrives at the cold heat exchanger compressing the gas isothermally. The compressed gas travels a small distance inwards the regenerator extracting heat from the regenerator wall due to its temperature gradient. As the wave travels further (away from the gas parcel), the heated compressed gas expands producing work, which results in an amplification of the wave. The expanded hot air travels back through the regenerator to its starting position, transferring its heat to the regenerator. When the wave is transported through the loop and arrives at the cold side, the cold air is compressed and the cycle starts again. Every cycle delivers work increasing the acoustic energy in the system.

2.5 Standing versus travelling wave systems

In order to maximise the amount of work per cycle on the gas the stack or regenerator porosity has to be very high while having a hydraulic radius small enough to ensure good thermal contact with the working gas. The hydraulic radius is an equivalent to the pore size and it is used to compare different pore geometries. It is defined as the ratio of the channel's cross-sectional area of the flow to its wetted perimeter [26]:

$$r_h = \frac{A_{pore}}{\Pi} \quad (1.13)$$

If the hydraulic radius is too large, the layers of gas away from the walls react adiabatically and do not contribute to the thermoacoustic effect. The hydraulic radius has to be balanced with the thermal penetration depth, the thickness of the gas layer which is exchanging heat with the regenerator wall and is defined as:

$$\delta_\kappa^2 = 2\alpha T \quad (1.14)$$

where T is the period of heat transfer which in this setup is the duration of half a cycle and α is the thermal diffusivity defined by μ / Pr with μ the dynamic viscosity and Pr the Prandtl number. The Prandtl number is the ratio of kinematic viscosity to thermal diffusivity. The thermal penetration depth can also be written as [28]:

$$\delta_\kappa^2 = \frac{2k}{\rho_m c_p \omega} \quad (1.15)$$

with k , ρ_m and c_p the thermal conductivity, density and specific heat capacity of the gas and ω the radial frequency.

The hydraulic radius and the thermal penetration depth are important quantities that determine the behaviour of the acoustic wave [27]:

If $\delta \gg r$ perfect thermal contact takes place during half an oscillation period causing displacement and heat exchange to take place simultaneously. The pressure and velocity amplitudes are in phase as illustrated in figure 2.9. The associated thermodynamic cycle is the Stirling cycle.

If $\delta < r$ imperfect thermal contact takes place in half a oscillation period. The gas near the wall is experiencing thermal contact, the gas near the centre of the pore is compressing and expanding adiabatically. There is a time delay between velocity and heat transfer. This results in a 90 degree phase difference in pressure and velocity amplitudes as illustrated in figure 2.10. The concerning thermodynamic cycle is the Brayton cycle.

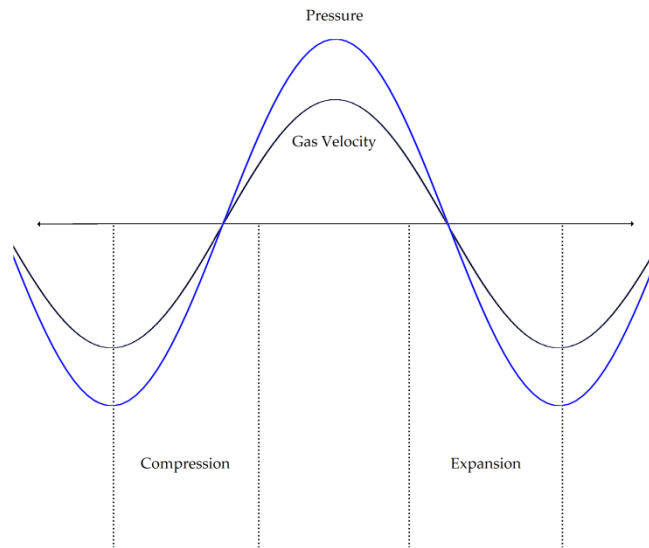


Figure 2.9: Plot of pressure and velocity for a travelling acoustic wave as a function of time, showing no phase difference between velocity and pressure.

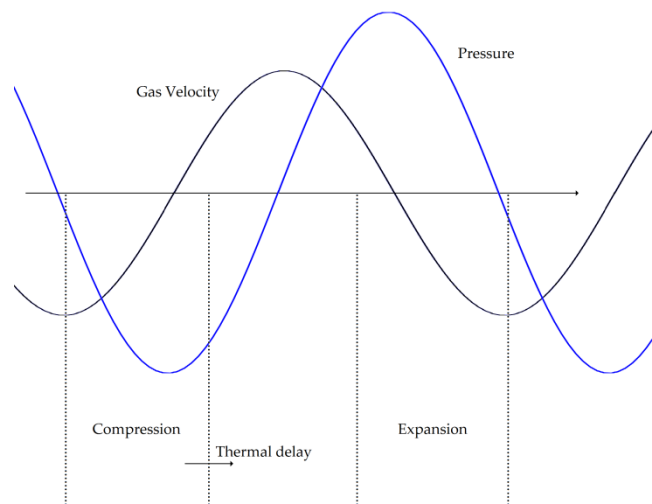


Figure 2.10: Plot of pressure and velocity for a standing acoustic wave as a function of time, showing 90° phasing between velocity and pressure.

2.5.1 Sound pressure

Sound pressure is the local pressure deviation from the mean pressure, caused by an acoustic wave. Sound pressure level or SPL is a logarithmic measure of the sound pressure relative to a reference value:

$$SPL = 20 \log_{10} \left(\frac{p_{\text{rms}}}{p_{\text{refer}}} \right) \quad (1.16)$$

with p_{rms} the root mean square or quadratic mean of the measured sound pressure and p_{refer} the reference sound pressure being $20 \mu\text{Pa}$.

2.5.2 Pressure ratio

Pressure ratio is an important parameter for evaluating the quality of a thermoacoustic system. It is defined as ratio of pressure amplitude to the mean pressure:

$$pr = \frac{|p|}{p_m} \quad (1.17)$$

Helium filled pressurized thermoacoustic systems can obtain high pressure ratios up to 1.40 [10].

2.5.3 Linearity

At high pressure ratios nonlinear effects will occur. Due to high particle velocities in the system friction will cause different forms of unwanted streaming that can reduce the systems efficiency. Nonlinear behaviour will already be significant at pressure ratios from 1.1% and over [11].

3. Design

In this chapter the design and construction of the thermoacoustic engine are presented. First, the requirements for the setup are discussed. Next the design considerations are discussed and drawings of the setup are presented. Finally the way of construction is shown with the use of pictures.

3.1 Requirements

The thermoacoustic prime mover will be designed according to a number of requirements:

1. A thermoacoustic travelling wave has to be observable.

Since travelling wave thermoacoustic engines have remarkably high overall efficiencies they are a promising technology for future applications. Therefore for the design of this thesis a travelling wave system is chosen. Transducers will be integrated in the system to obtain characteristics of the travelling wave.

2. The system must contain a multi stage engine setup.

A problem in most thermoacoustic systems is their high onset temperature and low power density. A multistage engine can have lower onset temperatures and higher power densities than single stage engines. For this reason a multistage setup is designed which can be adapted to a single stage design to compare its different outputs and efficiencies.

3. The thermoacoustic effect has to appear quickly.

Since the device will also be used to demonstrate the thermoacoustic effect, the start-up time for the system has to be short. An adjustable heat source has to be implemented in the system, so a high heat input can be selected to start resonance quickly.

3.2 Parts

3.2.1 Tube specifications

Since the experiments will include different stage setups, the thermoacoustic device has to be adjustable to both single stage and multistage configuration. The tube material has to be easy to adapt. For this reason metal loops, commonly used in thermoacoustic systems are not favourable for this design. PVC is chosen which is often a used material in small scale thermoacoustic systems. Refilling the system with helium or any other gas other than air after reconfiguration is a time consuming process. Therefore air at atmospheric conditions is chosen as a working gas.

The tube length is selected in a way the frequency of the system will operate in the range of 100 to 200 Hz since this is a commonly used frequency range for air filled thermoacoustic systems. A diameter of 45 mm is chosen since it is a widely used diameter in PVC built systems [12] [13] [14]. Due to the dimensions of the available PVC material with 45 mm diameter the minimal tube length will be 1.77 m regarding to a frequency 178 Hz.

3.2.2 Regenerator

The following requirements apply to the regenerator:

1. High porosity to provide high gas volume in the cycle to increase power density.
2. Small hydraulic radius to ensure good thermal contact between gas and regenerator.
3. Low conductive material to minimize conduction losses from hot to cold heat exchanger.

Two regenerator materials are commonly used: stainless steel in the form of wire mesh or ceramic material in the form of a squared catalyst. Ceramic regenerators can be easily made out of Diesel particulate filters (shown in figure 3.1) by removing the metal shell and cutting the ceramics in the cylindrical shape so it can be inserted in the regenerator tube. The pore width of common filters are 1 mm squared in geometry which equals a

hydraulic radius of 0.25 mm. For air at 1 atmosphere with a frequency of 178 Hz the thermal penetration depth is 0.35 mm which is larger than the hydraulic radius and provides therefore good thermal contact. The thermal conductivity of the ceramic catalyst is lower than the wire mesh thermal conductivity. Ceramic catalyst is chosen for this design, due to its good thermal contact, low thermal conductivity and availability.



Figure 3.1: *Ceramic catalyst used as regenerator material.*

3.2.3 Hot heat exchanger

In most thermoacoustic systems in practice heat is transferred to the system via a hot fluid such as thermal oil. In this experimental setup electric heating will be sufficient. An electric heater can be made out of electric wire from a range of conductive materials. However, the production of such an exchanger is a time consuming and therefore costly process. For this reason two ready to install 6.5 mm cartridge heaters¹ are chosen, suitable for variable heat generation up to 200 Watts each. The heat supply will be adjusted with the use of a variac. Both cartridge heaters will be placed parallel at one side of the regenerator. Heat is transferred to the regenerator by conduction through fins. Copper is chosen as fin material because of its high thermal conductive properties.

3.2.4 Cold heat exchanger

The cold side of the regenerator will be cooled by cooling water. This cold heat exchanger will consist of copper tubes, connected to the regenerator by copper foil fins.

¹ Schwedersky productnumber 120004, d 6.5mm, L 40mm, P max 200W

Heat will be extracted to maintain a regenerator temperature of 25°C. Heat is transferred to a 18°C water flow inside the tubes.

$$\rho_w A_t v = \frac{Q}{c_{p,w} \cdot \Delta T} \quad (1.18)$$

In order to reject up to 200 Watts of heat the water flow has to be 6.8 g/s. If three 2.4 mm internal diameter copper tubes are chosen, the water velocity has to be kept at 0.50 m/s.

3.2.5 Regenerator tube

The regenerator and heat exchangers are placed in the looped tube. However, PVC is not suitable as tube material here since the hot heat exchanger temperature exceeds the maximum PVC temperature of 80 °C. The regenerator tube has to meet the following requirements:

1. The tube must withstand temperatures up to 500 °C.
2. The effective conduction of the tube has to be low since conductive heat losses from hot to cold heat exchanger have to be minimized.

Glass, ceramics and low conductive metals are suited the regenerator tube materials. Stainless steel has the highest conductivity of the three, but since holes for the heat exchangers have to be milled it is a more suitable option than glass or ceramics. Using the lathe the tube thickness is brought down to 1.5 mm reducing its effective conductivity significantly. On both sides of the tube flanges are welded making the system airtight.

3.2.6 Stub

A stub was first introduced only two years ago, in 2012. It is a short side branch pipe that reduces backward travelling waves that cause a standing wave. The principle is illustrated in figure 3.2. As the travelling wave propagates through the loop it reaches the regenerator and is partly reflected. This wave travels in opposite direction with the same frequency. A near standing wave is created using superposition since the net displacement of the medium is the sum of the two waves.

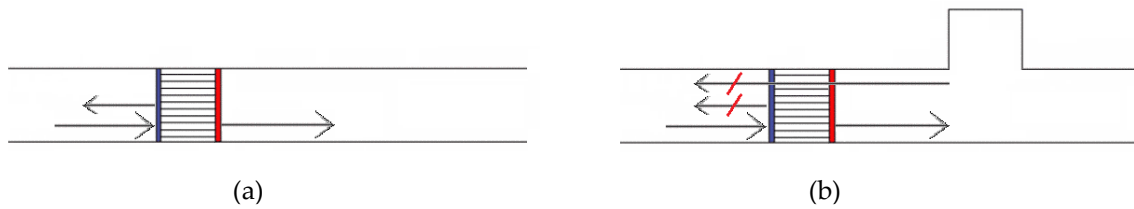


Figure 3.2: Illustration of a thermoacoustic system without and with the implementation of a stub. The travelling wave is partly reflected by the regenerator wall (a). This wave travels in opposite direction and a near standing wave is created using superposition. With the implementation of a stub this reflection is cancelled out so only the original traveling wave is present in the system (b).

These acoustic reflections can be cancelled out by adding an equal and opposite reflection from the side stub [23]. The hard wall at the end of the stub reflects the wave to the T-junction where some of the waves are sent backwards through the regenerator. This reflection cancels out the original reflection of the regenerator. More details about this principle are not described in literature and therefore it is not further discussed in this report.

The location of the stub should be close to the source of reflection, therefore the location is chosen to be right behind the regenerator. The length of the stub is determined during the experiments by varying the length of the side branch pipe with the use of a piston to find its optimum.

3.2.7 Alternator

Acoustic energy can be converted into electric power by the use of a linear alternator. An alternator contains a magnet that moves in relation to an electromagnetic coil and thus induces the flow of an electric current. In this setup the output power is order of magnitude of Watts. Therefore a loudspeaker is used. The speaker is selected according to its resonance frequency to match the 178 Hz base frequency of the system, an 8 Ohm loudspeaker with resonance frequency of 180 Hz is chosen².

² Visatron R10S 303648-89 max 30W

3.3 Construction

3.3.2 Regenerator tube

The regenerator tube is produced on the lathe according to the dimensions of figure 3.3. The inside diameter of stainless steel tube is increased to 45 mm on the lathe. Flanges are welded on both sides to connect to the PVC loop so that the system is airtight. Holes for the hot and cold heat exchanger are drilled using the lathe. For the hot heat exchanger the holes only have to be drilled at one side since the cartridge heaters are shorter than the inside diameter. In order to insert the heat exchanger fins over the hot heat exchanger which are located halfway the regenerator tube, the tube has to be made out of two parts that can be connected after the assembly of the heat exchanger. These two parts are connected by flanges. The flanges are turned, drilled and welded to the thin walled stainless steel pipe. The result is shown in figure 3.4.

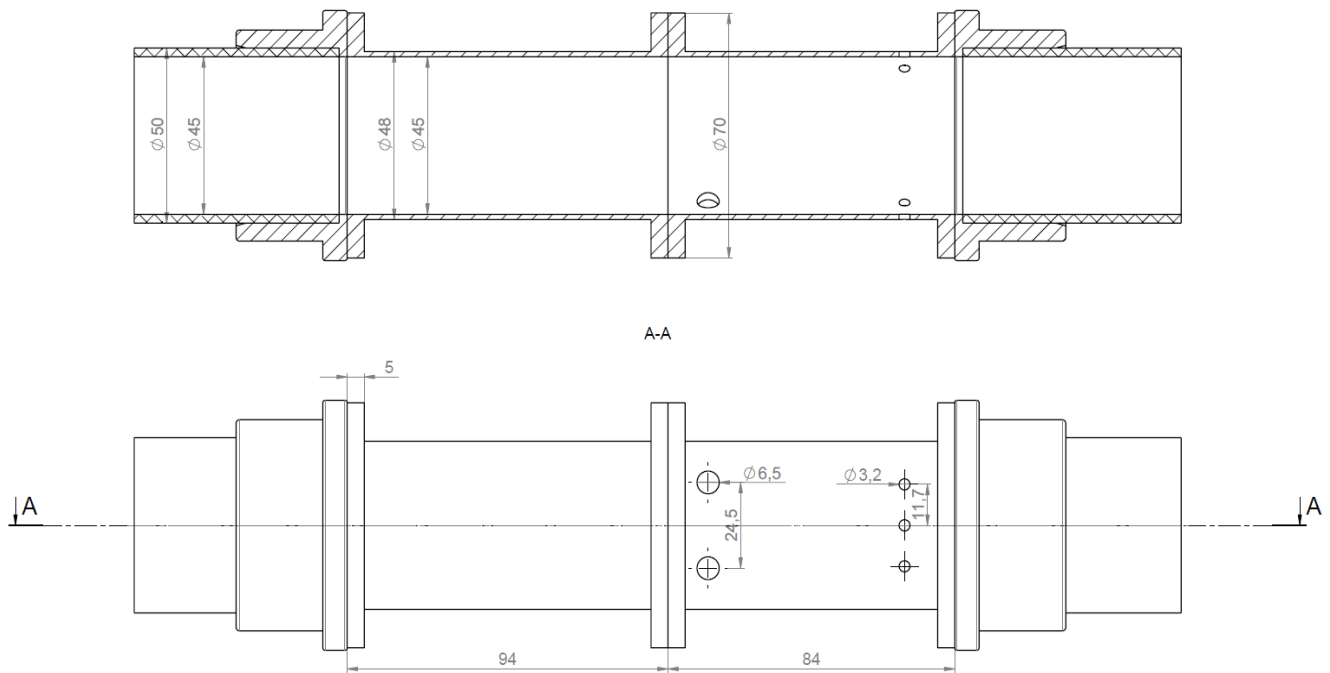


Figure 3.3: Drawings of the regenerator tube (mm).



Figure 3.4: *Assembly of the second regenerator tube.*

3.3.1 Regenerator

The ceramic regenerator is made out of the catalyst of a Diesel particulate filter. The catalyst is sawn into a 40 mm long 45 mm diameter cylinder, so that it fits precisely inside of the regenerator tube.

3.3.3 Hot heat exchanger

Copper foil is cut into 8.5 mm strips, folded around stainless steel plates of the same width, drilled and placed over the cartridge heaters inside the regenerator tube as shown in figure 3.5. The spacing between the layers of copper foil is 1.2 mm.

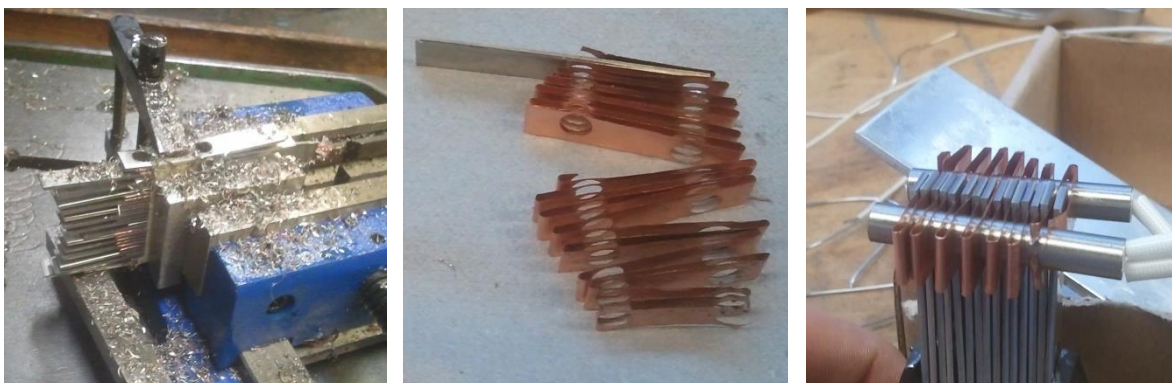


Figure 3.5: *Construction of the hot heat exchanger. A copper strip is wound around stainless steel plates, drilled and placed over the cartridge heaters.*

3.3.4 Cold heat exchanger

Three copper tubes of 3.2 mm outside diameter and a thickness of 0.4 mm are placed parallel, 5 mm copper foil is drilled and placed over the tubes touching the regenerator to ensure proper heat conduction from the regenerator to the water flow as shown in figure 3.6.



Figure 3.6: *Construction of the cold heat exchanger.*

3.3.5 Assembly

The constructed parts are assembled according to figure 3.7. The PVC parts are glued together except for one side of the PVC coupling because the second stage of the engine has to be replaceable with an ordinary tube of single stage configuration (figure 4.1).

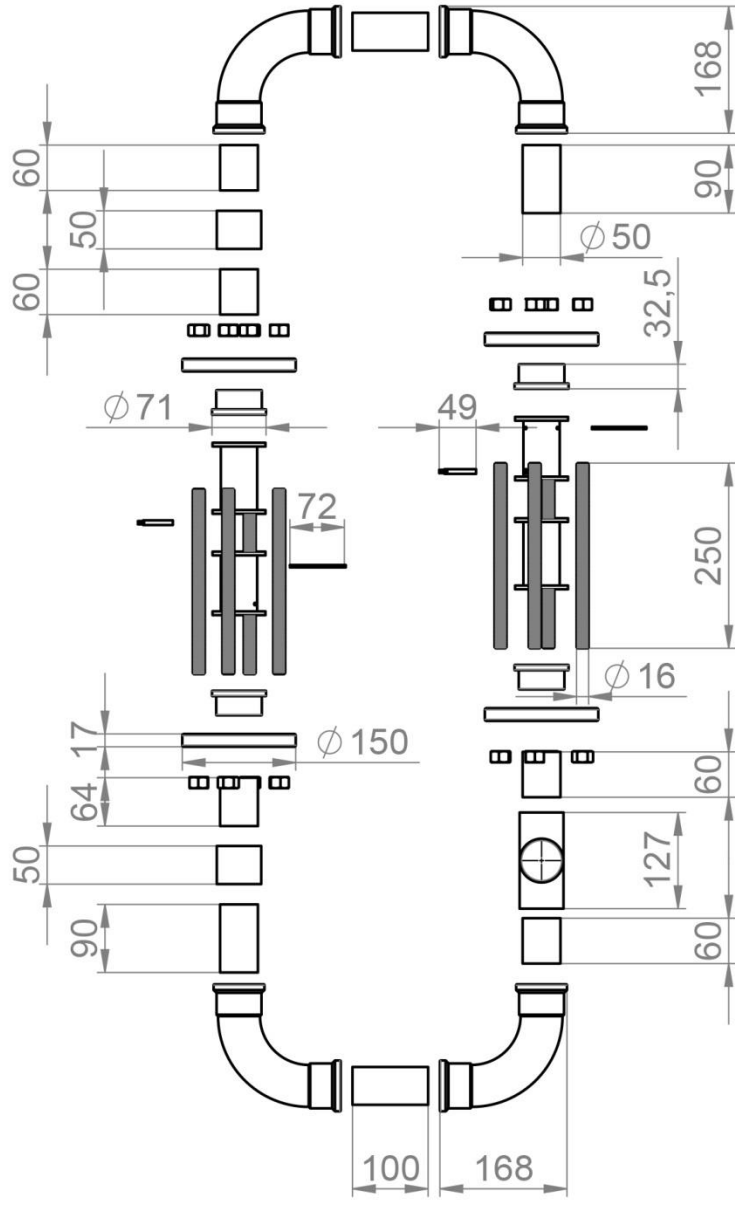


Figure 3.7: Dimensions of the tube parts in mm and its assembly order of the thermoacoustic prime mover in double stage configuration, scale 1:10.

4. Experimental results

4.1 Experimental setup

The result of the assembly is shown in figure 4.1. The thermoacoustic stage next to the stub is permanent, the opposite stage can be replaced by a PVC tube, inserted in the loop in coupling slips.

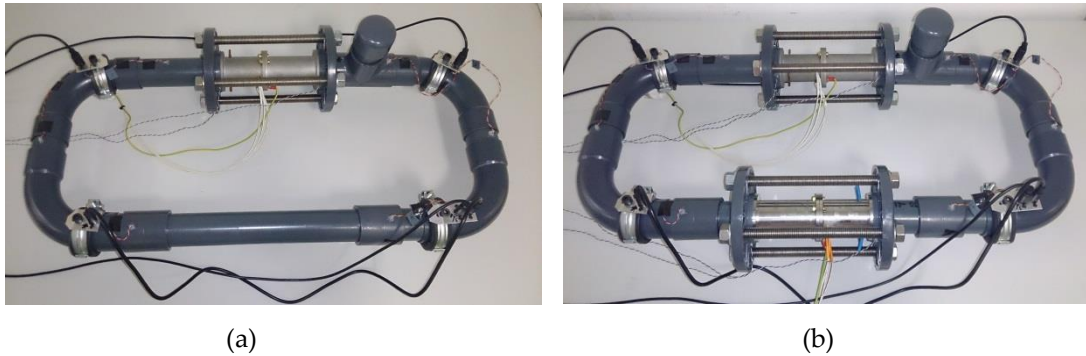


Figure 4.1.: *Experimental setup in single stage configuration (a) and double stage configuration (b).*

4.2 Data acquisition

4.2.1 Temperature measurements

Regenerator temperature measurements are done with the use of J-type thermocouples³. The thermocouples are inserted in both sides of the regenerators, and are connected to a thermocouple input device⁴, which output is sent to a computer. The program LabVIEW is used to acquire the data.

4.2.2 Acoustic pressure measurements

Acoustic pressure measurements are done by Sonion microphones⁵. Six microphones are placed in the tube wall at the locations presented in figure 4.2. The

³ RS № 621-2142 (max 750 °C)

⁴ NI USB-9162, C-Series Single Module Carrier

⁵ Sonion 8040 (@1.3 VCD: sensitivity -44 dB re. 1V/Pa, max input level 130.5 dB)

signals are amplified and sent to data acquisition device⁶ connected to a computer. The data is acquired by LabVIEW.

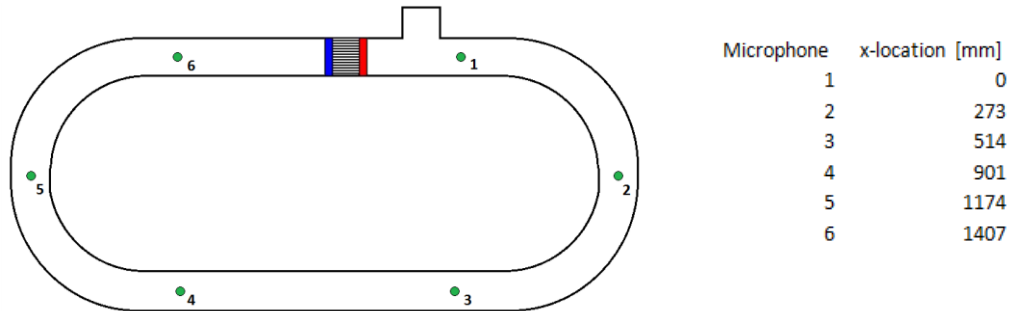


Figure 4.2: Schematic illustration of the experimental setup along with the x-locations of the microphones.

The calibration is done by a pistonphone. A pistonphone is a device that uses a closed coupling volume to generate a precise pressure wave for calibration. Inside the device a piston is mechanically driven to move at a specific frequency, pushing on a fixed volume to which the microphone is coupled. The known Sound Pressure Level can be related to an output voltage of the microphone. The pistonphone used in this setup⁷ operates at 250 Hz at a Sound Pressure Level of 114 dB.

4.2.3 Electric power output and efficiency

The loudspeaker is connected to a variable resistance with a maximum of 8 Ω . A multimeter is used to determine the equivalent resistance and to measure the output voltage. The system overall efficiency is calculated by:

$$\eta = \frac{\dot{E}_{el}}{Q_{in}} \quad (1.19)$$

where $\dot{E}_{el} = \frac{U^2}{R}$.

⁶ NI USB-6009, 14-Bit 48 KS/s

⁷ G.R.A.S. 42AA

4.3 Results

In this section the results of the experiments with the thermoacoustic prime mover are presented. First the results of the single stage setup are discussed in terms of onset temperature, onset time, phase difference and a frequency analysis. Second the results of the double stage prime mover are presented and compared with its single stage configuration.

4.3.1 Single stage prime mover

4.3.1.1 Temperature

In order to bring a thermoacoustic prime mover into resonance a minimal heat input as to be implemented on the system. This heat input varies for different devices. In this section the minimal heat input to bring the experimental setup in resonance is determined.

First the system is brought to resonance using a high heat input of 120 Watts. Next the heat input is decreased slowly until resonance fades out. This happens at a heat input of just under 44 Watts making 44 Watts the minimal heat input to keep the system in resonance.

Now the onset temperature is determined. The onset temperature of the system is an important quantity for the quality of a thermoacoustic device. Low onset temperature engines can be implemented in a wider range of applications. In particular in waste heat recovery systems a low system onset temperature is required. The engines onset temperature is determined by supplying the 44 Watts minimal heat input to the system. The temperature of the hot and the cold side of the regenerator are plotted in figure 4.3 as a function of time.

At minimal heat input oscillation starts at 26.3 minutes. Of course the startup time of the engine can be much shorter by implementing a higher heat input to the system. The onset temperature is 303 °C As the thermoacoustic engine produces work by transferring heat from the hot to the cold side, a sudden decrease in temperature at the hot side and an increase in temperature at the cold side of the regenerator occur. The

temperature gradient decreases. When the temperature gradient drops below the critical temperature no more heat is converted into acoustic energy and the resonance fades out.

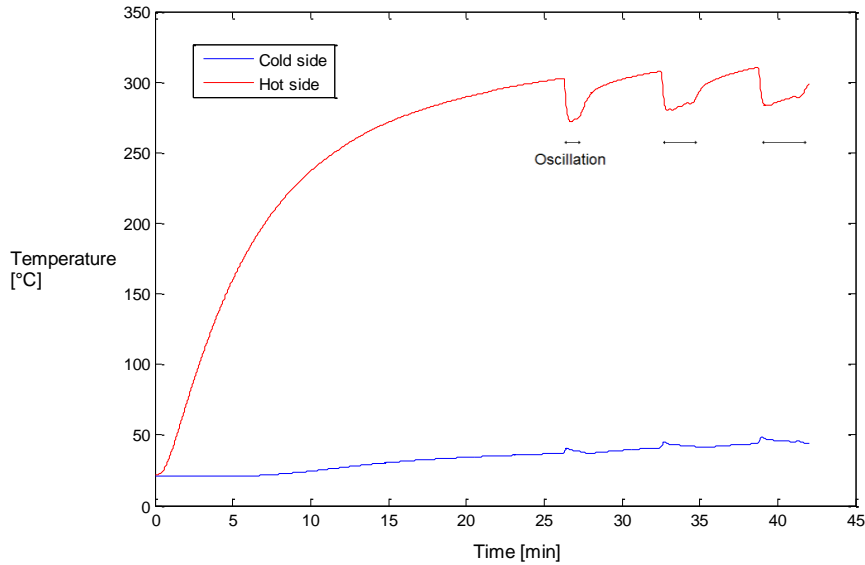


Figure 4.3: Temperature at both sides of the regenerator as a function of time at 44 Watts heat input.

However, heat is continued to be supplied to the system with a magnitude of 44 Watts. The hot side increases in temperature again until the temperature gradient exceeds the critical temperature gradient and oscillation is restarted at 34.7 minutes. Note that the onset temperature at this oscillation period equals 307 °C, an increase of 4 °C. This can be explained by the fact that the cold side of the regenerator has also increased 4 °C in temperature, an increase that has to be compensated by the hot side in order to maintain critical temperature gradient.

The oscillation period is shown with a black line in figure 4.4. It can easily be seen that the oscillation period increases every time oscillation starts. This is because more and more heat is captured by the engine material which is getting close to its working temperature, so more heat becomes available for acoustic energy generation. At first when the cold engine is turned on, the total amount of heat supplied to the engine is used to heat up the components. When these components have reached their working temperature, the heat supply is enough to both maintain their temperature and generate acoustic energy and oscillation will not fade out anymore.

4.3.1.2 Pressure

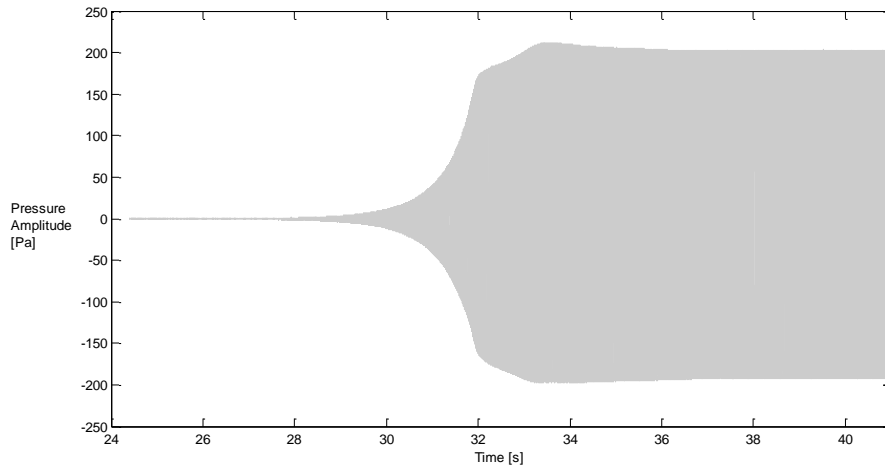


Figure 4.4: Onset pressure deviation from the ambient atmospheric pressure at an input of 80.3 Watts of heat.

The heat input increased to 80.3 Watts. Figure 4.4 shows the onset pressure behavior from the moment oscillation starts. As oscillation starts the sound wave is amplified every thermoacoustic cycle. Within a second the pressure amplitude has reached its maximum value, and decreases to its steady state value of 203 Pa at 80.3 Watts of heat input.

Figure 4.5 shows the pressure waves at six points in the tube at 80.3 Watts heat input with a damped resonator. The reason the resonator is damped is to keep the pressure amplitudes in the low measuring range of the microphones. Since the measuring range is limited by a maximum of 130.5 dB a pressure deviation of 16 Pa is chosen corresponding to 118 dB SPL. The phase differences indicate the presence of a travelling wave. Interesting is the large difference in pressure amplitudes. A probable cause for this is that next to a travelling wave also a standing wave may be present. In order to ensure only a travelling wave is moving through the engine, a regenerator with a smaller hydraulic radius can be selected to further increase thermal contact.

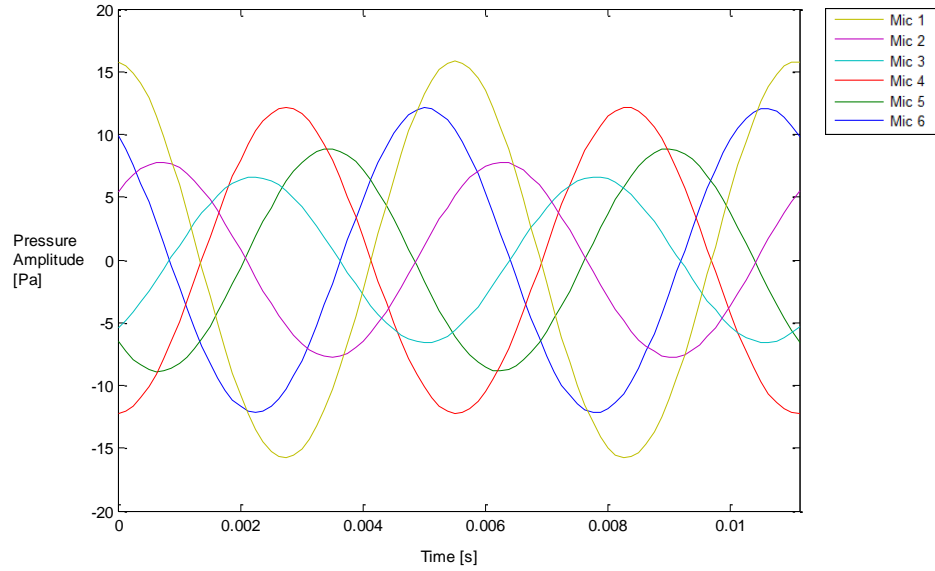


Figure 4.5: Pressure waves at different points in the engine at an input of 80.3 Watts with a partially closed resonator.

The power spectral density plot up to 1000 Hz is presented in figure 4.6. The base mode is clearly visible at 180 Hz as well as two higher harmonics of the base mode at 360 Hz and 550 Hz. Higher harmonics are unwanted since acoustic power can only be harvested from the base mode, acoustic energy is converted to electricity with the use of a linear alternator operating at the fundamental frequency. Higher frequencies do not contribute to the movement of the alternator. At standing wave systems the acoustic

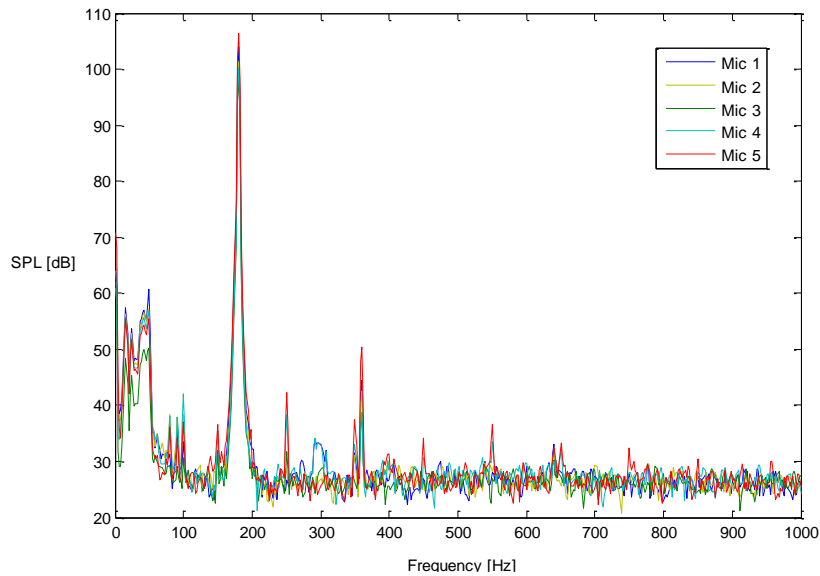


Figure 4.6: Power spectrum at an input of 80 Watts with a partially closed resonator.

power of the higher harmonics can be 60% of the total acoustic power and are therefore major losses [24]. When the cross sectional area is constant throughout the entire length of the resonator the harmonics are multiple integers of the fundamental causing the harmonics to coincide with resonance frequencies and get amplified. However, when inserts are added to the resonator higher harmonics are still generated but not as integer multiples of the fundamental frequency. This reduces the amplitude of the higher harmonics [25]. The acoustic power of the base frequency can be increased with 160% [24]. In this experimental setup the sound pressure level of the base mode is a factor 650 higher than the second harmonic and therefore no harmonics suppression is needed.

4.3.2 Single stage versus double stage prime mover

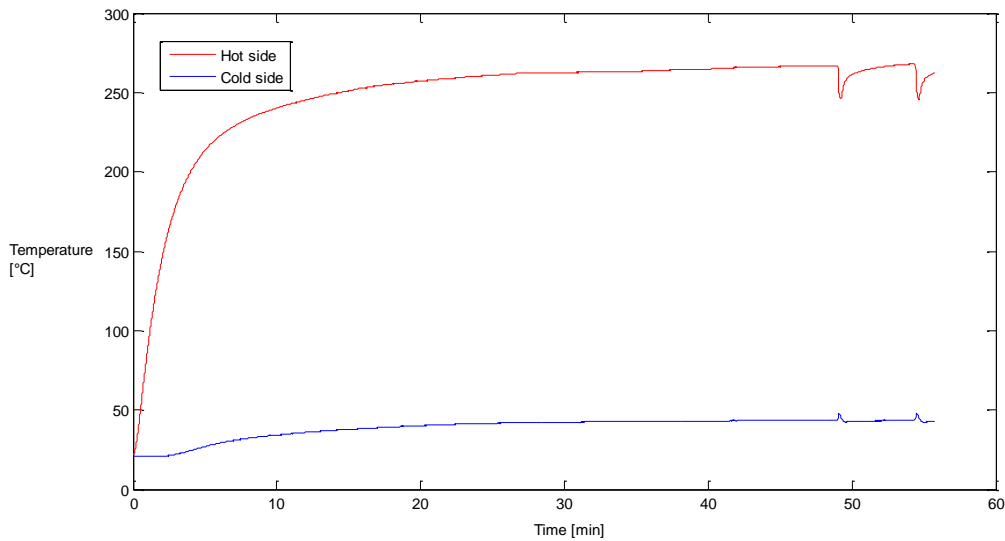


Figure 4.7: Temperature onset behaviour of the double stage prime mover at 60 Watts of heat input. Both hot and cold site temperatures are averages of the two hot and the two cold sides of the regenerator.

For the double stage thermoacoustic engine the minimal heat input to work is determined to be 60 Watts. When the engine is cooled down and the heat is supplied it takes 49 minutes to start resonance with an onset temperature of 267 °C as shown in figure 4.7. This onset temperature is significantly lower than the onset temperature of the single stage prime mover which was 303 °C. There is more heat input needed to

bring the system into resonance since two stages have to be increased in temperature. However, a 36 °C lower onset temperature can be interesting for applications which main requirement is a low onset temperature. An example is waste heat recovery, an application where a large energy flow is present at a low temperature. This shows multistage engines are favorable on that domain.

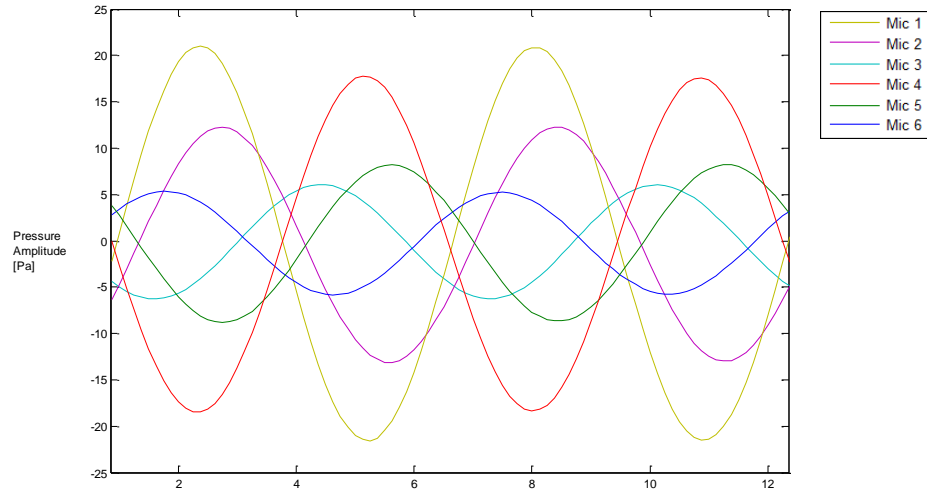


Figure 4.6: Pressure waves for a double stage engine at different points at an input of 103 Watts with a partially closed resonator.

In figure 4.6 the pressure behavior of the double stage engine is presented. Since it contains two stages, the total heat provided to turn the system into resonance is higher than for the single stage engine. Therefore the pressure measurements are done at 103 Watts power input. Since the measuring range of the microphones is limited by 130.5 dB the resonator damped giving a maximal pressure amplitude of 21 Pa (120.4 dB).

Figure 4.8 and 4.9 show respectively the electric power output and the overall efficiency for both single and double stage configuration as a function of heat input. The results show the electric power output seems to increase linearly with heat input. The double stage prime mover can convert a much higher input power because of its lower operating temperature so a higher electric power can be realized. This increases the

engines power density tremendously which is required in large scale thermoacoustic systems.

The efficiency of the single stage prime mover is higher than the efficiency of the double stage prime mover at any input in the experiments. The 2nd law efficiency is at least 34% higher at any heat input under 150 Watts.

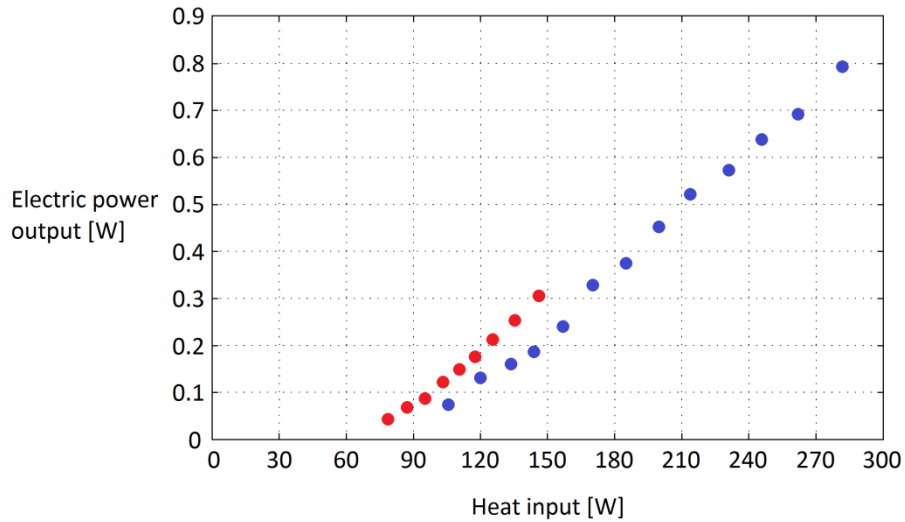


Figure 4.8: Electric power output as a function of total heat input for single stage (●) and double stage (●) configuration.

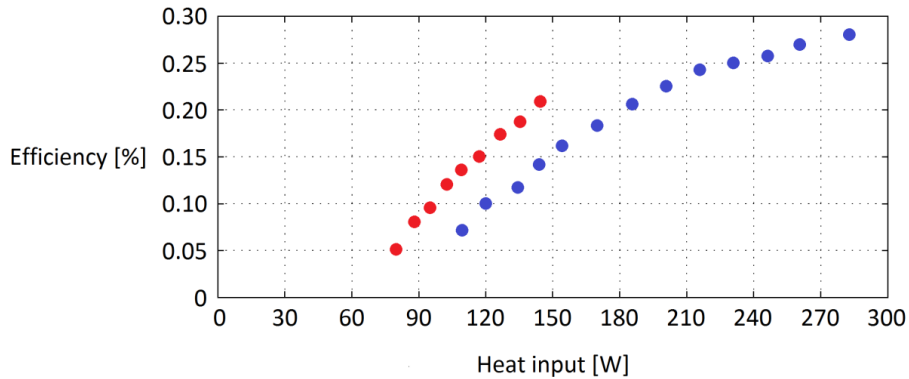


Figure 4.9: Overall efficiency as a function of total heat input for single stage (●) and double stage (●) configuration.

5. Conclusions and recommendations

A thermoacoustic prime mover was designed and build using air at 1 atmosphere as a working fluid. The regenerators were heated using electricity and cooled using cooling water. Pressure and temperature measurements are done at several locations in the engine. It has been shown that acoustic energy can be converted into electric power with the use of a linear alternator. It has also been shown that the double stage engine operates at a lower working temperature, it can produce more electric power and thus obtains a higher power density than the single stage thermoacoustic engine. Measurements show the onset temperature of the single and double stage engine are respectively 303 °C and 267 °C. However, 2nd law efficiencies for single stage configuration are at least 34% higher than efficiencies for double stage configuration. An electric output power of 0.79 W is realized at an overall efficiency of 0.28%.

Several adjustments are recommended to the design to ensure a higher overall efficiency:

1. To eliminate the presence of a standing wave a regenerator with a smaller hydraulic radius can be selected, or the systems base frequency can be lowered.
2. The cold side of the regenerator was designed to maintain a temperature of 25 °C. However, cold side regenerator temperatures went up to 40 °C decreasing the engines efficiency. In order to improve the thermal to acoustic efficiency more fins have to be implemented in the cold heat exchanger providing better conduction between the cooling water tubes and the regenerator.
3. A regenerator tube with a lower thermal conductivity can be selected to prevent conduction losses from the hot to the cold heat exchanger improving thermal to acoustic efficiency. In the current setup a thin walled stainless steel regenerator tube is used, alternative low conduction tube materials can be ceramics or glass.

Bibliography

- [1] K. Sondhauss, "Über die Schallschwingungen der Luft in erhitzten Glasrohren und in gedeckten Pfeifen von ungleicher Weite", *Annalen der Physik und Chemie*, vol. 79, pp. 1-34, 1850.
- [2] B. Higgins, *Journal of Natural Philosophy and Chemical Arts*, vol. 129, p. 22, 1802.
- [3] P. L. Rijke, "On the vibration of the air in a tube open at both ends," *Philosophical Magazine*, vol. 17, pp. 419-422, 1859.
- [4] B. Rayleigh, *Theory of Sound*, New York: Dover, 1945.
- [5] H. Kramers, "Vibrations of a gas column," *Physica*, vol. 15, p. 971, 1949.
- [6] G. Kirchhoff, "Ueber den Einfluss der Wärmeleitung in einem Gas auf die Schallbewegung," *Annalen der Physik*, vol. 134, p. 177, 1868.
- [7] N. Rott, "Thermoacoustics," *Advances in Applied Mechanics*, vol. 20, pp. 135-175, 1980.
- [8] T. Hofler, "Thermoacoustic refrigerator design and performance," Physics dep. University of California, San Diego, 1986.
- [9] G. W. Swift, *A unifying perspective for some engines and refrigerators*, Melville: Acoustical Society of America, 2002.
- [10] G. Yu, E. Luo, W. Dai. and Z. Wu, "An energy-focused thermoacoustic-Stirling heat engine reaching a high pressure ratio above 1.40," *Elsevier*, vol. 47, no. 2, pp. 132-134, 2007.
- [11] A. A. Atchley, *Annual summary of basic research in thermoacoustic heat transport*, Monterey: Naval Postgraduate School, 1990.
- [12] K. de Blok, "Demonstration of the thermoacoustic water heater-generator," *Aster Thermoacoustics*, 28 11 2012. [Online]. Available: <http://www.aster-thermoacoustics.com/?p=894>.
- [13] J. H. Wilmink, "Thermoacoustic traveling wave heat engine: modeling and experimental validation," University of Twente, Enschede, 2013.
- [14] I. Setiawan and A. B. Setio-Utomo, "Experimental Study on Thermoacoustic Cooling System with Two Stacks in a Straight Resonator Tube," in *10ème Congrès Français*

d'Acoustique, Lyon, 2010.

- [15] U. E. I. Administration, "International Energy Outlook 2013," Washington DC, 2013.
- [16] S. Spoelstra, "Thermoacoustic systems," ECN, 02 August 2007. [Online]. Available: <https://www.ecn.nl/fileadmin/ecn/units/eei/Onderzoeksclusters/Restwarmtebenutting/b-07-006.pdf>. [Accessed 30 June 2014].
- [17] V. Smil, *Energy Transitions: History, Requirements, Prospects*, Praeger Publishers, 2010.
- [18] "Qnergy set a new world record," Qnergy, 30 April 2014. [Online]. Available: <http://www.qnergy.com/qnergy-set-a-new-world-record->. [Accessed 30 June 2014].
- [19] B. Chen, A. A. Yousif, H. R. Paul and B. H. David, "Development and Assessment of Thermoacoustic Generators Operating by Waste Heat from Cooking Stove," 1 October 2012. [Online]. Available: <http://dx.doi.org/10.4236/eng.2012.412113>. [Accessed 30 June 2014].
- [20] P. Perrot, *A to Z of Thermodynamics*, Oxford: Oxford University, 1998.
- [21] P. Guillaume, G. Matthieu and G. Vitalyi, "Account of heat convection by Rayleigh streaming in the description of wave amplitude growth and stabilization in a standing wave thermoacoustic prime-mover," in *International Symposium on Nonlinear Acoustics*, Maine, 2012.
- [22] A. Ibrahim, H. Omar and E. Abdel-Rahman, "Constraints and challenges in the development of loudspeaker driven thermacoustic refrigerators," in *International congress on sound & vibration*, Rio de Janeiro, 2011.
- [23] Z. Yu, A. Jaworski and S. Backhaus, "Traveling-wave thermoacoustic electricity generator using an ultra-compliant," *Applied Energy*, vol. 99, pp. 135-145, 2012.
- [24] J. Liu, "Characterization of porous material used for thermoacoustic devices," The Pennsylvania State University, Pennsylvania, 2005.
- [25] P. in 't panhuis, *Mathematical Aspects of Thermoacoustics*, Eindhoven: Print Service Technische Universiteit Eindhoven, 2009.
- [26] G. W. Swift and P. S. Spoor, "Thermal diffusion and mixture separation in the acoustic boundary layer," Los Alamos National Laboratory, Los Alamos, 1999.

